Bioorganic & Medicinal Chemistry Letters 18 (2008) 5487–5492

Contents lists available at ScienceDirect

Bioorganic & Medicinal Chemistry Letters

journal homepage: www.elsevier.com/locate/bmcl

Imidazoles: SAR and development of a potent class of cyclin-dependent kinase inhibitors

Malcolm Anderson, David M. Andrews, Andy J. Barker, Claire A. Brassington, Jason Breed, Kate F. Byth †, Janet D. Culshaw, M. Raymond V. Finlay, Eric Fisher, Helen H.J. McMiken, Clive P. Green *, Dave W. Heaton, Ian A. Nash, Nicholas J. Newcombe, Sandra E. Oakes, Richard A. Pauptit, Andrew Roberts, Judith J. Stanway, Andrew P. Thomas, Julie A. Tucker, Mike Walker, Hazel M. Weir

AstraZeneca, Alderley Park, Macclesfield, Cheshire SK10 4TG, UK

ARTICLE INFO

Article history:
Received 7 August 2008
Revised 3 September 2008
Accepted 5 September 2008
Available online 10 September 2008

Keywords:
CDK
Kinase
Inhibitor
Cancer

ABSTRACT

An imidazole series of cyclin-dependent kinase (CDK) inhibitors has been developed. Protein inhibitor structure determination has provided an understanding of the emerging structure activity trends for the imidazole series. The introduction of a methyl sulfone at the aniline terminus led to a more orally bioavailable CDK inhibitor that was progressed into clinical development.

The process of cell division is a basic requirement for the assembly and survival of any multicellular organism. Normal progression through the cell cycle, leading to cell division, is a remarkably ordered process that is strictly coordinated and regulated by cyclin-dependent kinases (CDK) and their cyclin partners.[1] For example, the CDK2/cyclin E complex contributes to pRb phosphorylation to enable the G1/S-phase transition and activate the transcription factor E2F.[2] The CDK2/cyclin A complex then promotes uninterrupted passage through the S-phase and appropriately timed deactivation of E2F.[3] Studies using a dominant negative CDK2 have shown that CDK2 also has a role in entry to the G2/M-phase.[4]

Extensive profiling of tumour tissue has repeatedly identified components of the CDK signaling pathway that are altered in cancer.[2,5] This commonly occurs through amplification of cyclin effectors such as cyclins D and E, the inactivation of endogenous inhibitors such as p16 and p27, or genetic mutations to CDK substrates.[6,7] Due to such observations, CDKs are generally regarded as attractive targets for therapeutic intervention in cancer.[8]

In earlier communications, we described the invention of imidazo[1,2-*a*]pyridine (**1**) and imidazo[1,2-*b*]pyridazine (**2**) CDK inhibitors (Fig. 1).[9–12] Our desire was to find an alternative series of CDK inhibitors with improved physicochemical properties and/or increased cellular potency.[13] Our objective was ultimately achieved by use of a substituted imidazole in place of the bicyclic heterocycle and by use of a sulfone in place of the sulfonamide. This series of CDK inhibitors (**3**) was believed to be less lipophilic, as desired, and the initial examples exhibited similar levels of potency to the compounds of series (**1**) and (**2**) (Table 1).[9,10,14]

The preparation of the imidazole compounds (**4**) started with benzylation of 2-methyl-1*H*-imidazole-4-carbaldehyde **A**, which gave a mixture of benzyl-imidazoles **B** (Scheme 1). Addition of methylmagnesium bromide to the mixture and removal of the benzyl groups gave the alcohol **C**, which was oxidized to give the ketone **D**. Treatment with DMF-DMA installed the enamine and selectively methylated the desired nitrogen. Conversion of the aminopropenones **E** to the sulfonamides (**4**) exploited chemistry that had previously been used for the imidazo[1,2-*a*]pyridine series (Scheme 2).[9,10]

Imidazole rings bearing different substituents were prepared by first appending the R^3 group to the amino-isoxazoles **H** (Scheme 3).[15] Acylation of the amino-isoxazoles **I** then gave the amides **J**. These underwent hydrogenation, followed by base-assisted cyclization to give the methyl ketones **K**. Treatment with DMF-DMA gave the aminopropenones **L**. Conversion to the sulfonamides (**5**) used analogous sequences to those described in Scheme 2.

The biological results showed that variation of the 3-substituent (R^3) and 5-substituent (R^4) of the imidazole ring had more impact on enzyme potency than variation of the 2-substituent (R^2, data

* Corresponding author. Tel.: +44 1625 517526; fax: +44 1625 516667.
E-mail address: clive.green@astrazeneca.com (C.P. Green).
† Present address: AstraZeneca, 35 Gatehouse Drive, Waltham, MA 02451, USA.

0960-894X/$ - see front matter © 2008 Elsevier Ltd. All rights reserved.
doi:10.1016/j.bmcl.2008.09.024

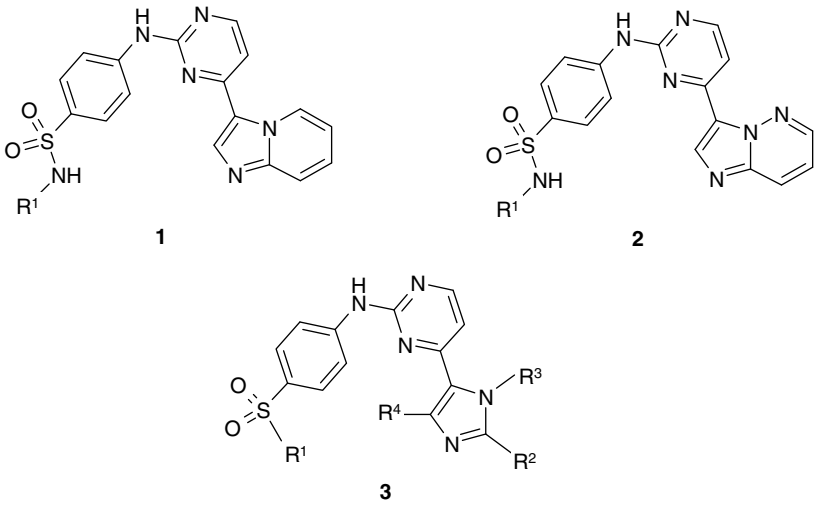

Figure 1. Small molecule CDK inhibitors.

Table 1
Structures and in vitro activity for imidazo[1,2-*a*]pyridines 1, imidazo[1,2-*b*]pyridazines **2** and imidazoles **4**

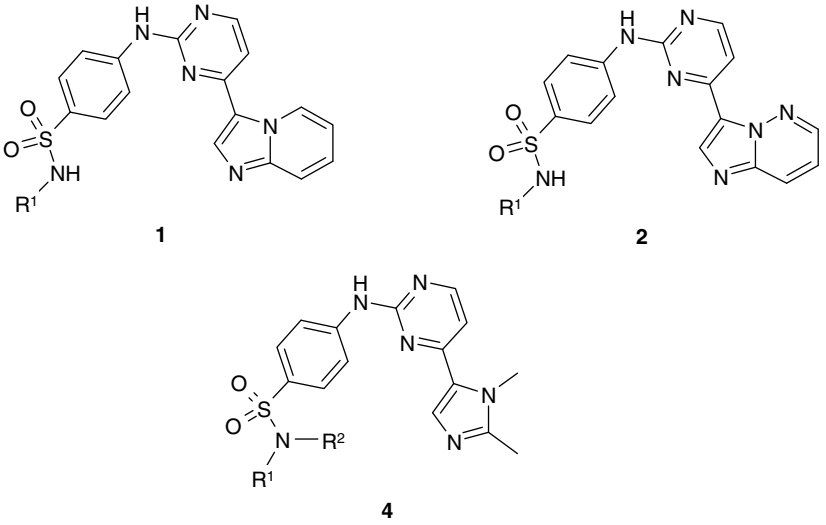

Compound	R^1	R^2	CDK2 IC_{50}[a] (μM)	MCF-7 prolif. IC_{50}[b] (μM)
1a	H		0.002	0.26
1b	$(CH_2)_2OMe$		<0.012	0.40
2a	Me		<0.003	0.56
2b	$(CH_2)_2N(Me)_2$		0.008	0.26
4a	H	H	0.011	0.87
4b	Me	H	<0.003	0.50
4c	$(CH_2)_2OMe$	H	0.008	0.62
4d	$(CH_2)_3O^iPr$	H	0.006	0.32
4e	$(CH_2)_2N(Me)_2$	H	0.025	0.49
4f	$(CH_2)_2OMe$	Me	0.40	

[a] Enzyme protocol Ref. 14.
[b] IC_{50} for inhibition of BrdU incorporation to MCF-7 cells following 48 h exposure to test compound.

not shown), possibly due to the lack of conserved residues in this region of the protein. Hence, the 2-substituent was retained as a methyl group during investigations of substitution at the 3-, and 5-positions (Table 2). The most significant potency improvements tended to be with α-branched substituents (compare **5b** and **5c** with **4c**, **5a** and **5d**), although ^{c}Pr was an outlier in this sequence (compare **5e** with **5b**). Formation of a tetra-substituted imidazole reduced activity (compare **5f** with **4c**). The compounds display selectivity for CDK2 over CDK4 and ligand efficiency comparable to the imidazo[1,2-*a*]pyridines (e.g. **5b** ligand efficiency 0.40).[9,10,16]

We undertook structural studies to investigate the binding-mode of the imidazoles when complexed to CDK2. The crystal structure of CDK2 complexed with **5b** (Fig. 2) shows that it binds at the ATP-binding site and that the imidazole ring adopts a binding-mode similar to that of the imidazo[1,2-*a*]pyridines.[9] The key hydrogen bonding interactions in the hinge region of CDK2 be-

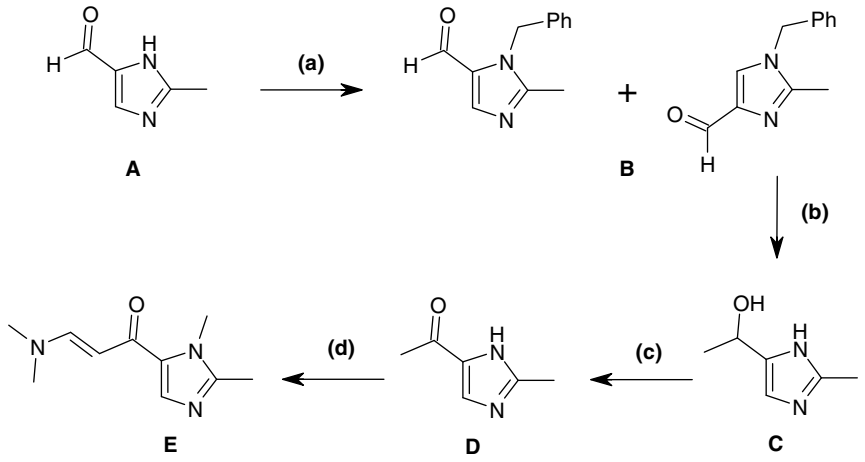

Scheme 1. Synthesis of aminopropenones **E**. Reagents and conditions: (a) K_2CO_3, BnBr, DMF, 0–20 °C, 2 h, 66%; (b) i—MeMgBr, THF, 0–20 °C, 18 h, 41%; ii—Pd/C, cyclohexenone, IPA, reflux, 3 h, 99%; (c) MnO_2, $CHCl_3$, reflux, 3 h, 75%; (d) DMF-DMA, DMF, 130 °C, 18 h, 46%.

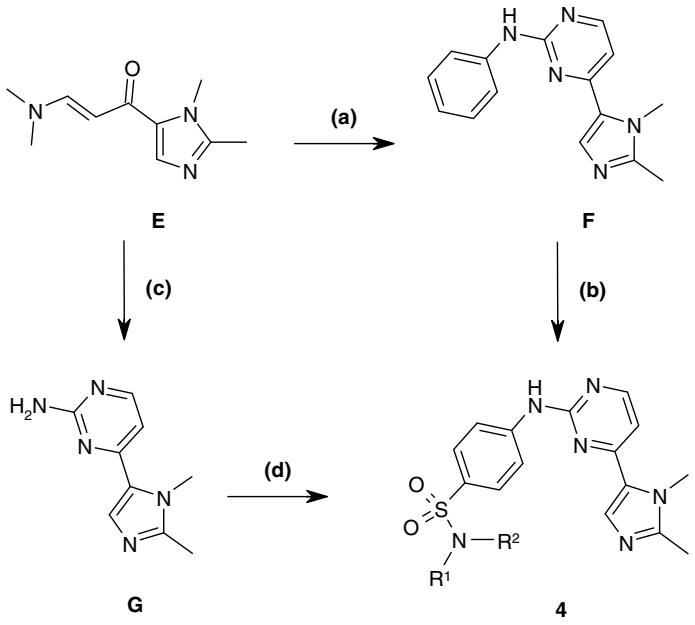

Scheme 2. Synthesis of imidazoles **4**. Reagents and conditions: (a) phenyl-guanidine hydrogencarbonate, NaOMe, DMA, 150 °C, 24 h, 96%; (b) i—$ClSO_3H$, $SOCl_2$, 0 °C-reflux, 1 h; ii—R^1R^2NH, MeOH, 0–20 °C, 18 h, 44–81% (2 steps); (c) guanidine hydrochloride, NaOMe, ^{n}BuOH, reflux, 18 h, 84%; (d) 4-I-C_6H_4-$SO_2NH(CH_2)_2OMe$, $Pd_2(dba)_3$, BINAP, NaO^{t}Bu, dioxane, 80 °C, 18 h, 84%.

tween Leu83 NH and the pyrimidine N, and between Leu83 O and the aniline NH are preserved. Similarly, the sulfonamide group retains hydrogen bonds with the carboxylic sidechain of Asp86 and the NH of Lys89.

The good activity of the R^3-alkylimidazoles could be attributed to the projection of the R^3 substituent into a hydrophobic region in the ATP-ribose binding domain that can accept appropriately sized lipophilic groups. The α-branched substituents appear to be very good for exploiting these hydrophobic contacts with the glycine-rich loop, in particular the interaction with the peptide backbone around Gly11 and the side chains of Ile10 and Val18. We postulate that steric bulk of the R^4 group (**5f**) increases the dihedral angle between the imidazole and pyrimidine rings, orienting the R^3 group away from the hydrophobic pocket and reducing the activity.

We also generated the X-ray structure of the ^{c}Pr derivative (**5e**) complexed with CDK2 (Fig. 3). Similar hydrogen bonding interactions to those observed for **5b** were again identified, but orientation of the imidazole ring is inverted and the binding-mode resembles that of the imidazo[1,2-*b*]pyridazine CDK inhibitors.[11] This removes the water-mediated interaction between the imidazole N and Asp145 of **5b** and allows the ^{c}Pr group to access the shallow cavity at the back of the ATP-binding cleft that is defined by the side chain of Phe80. The ^{c}Pr group forms a hydrophobic edge-to-face interaction with this residue and desolvates the hydrophobic surface in this region.

The combination of cellular potency and physicochemical properties of the imidazole CDK inhibitors required further optimization to identify orally active agents and we sought to modify these compounds to remove the weakly acidic secondary sulfonamide group. We reasoned that good enzyme potency could still be achieved in the absence of the hydrogen bonding interaction with the carboxylic sidechain of Asp86 providing

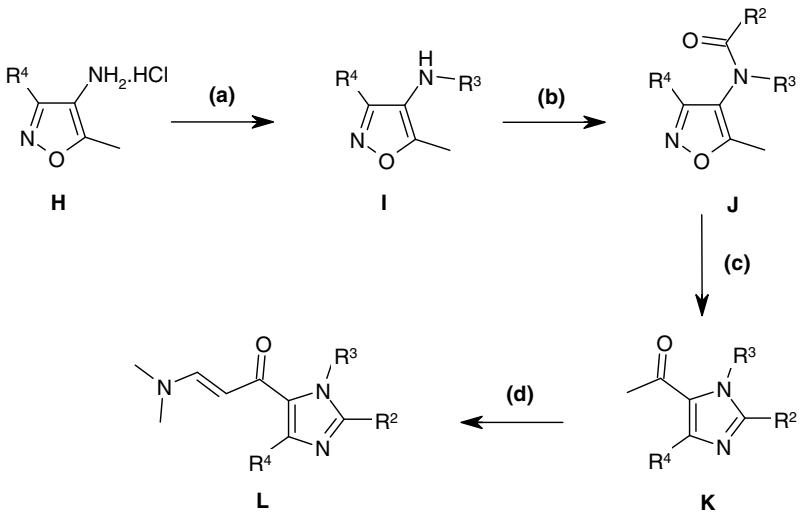

Scheme 3. Synthesis of aminopropenones **L**. Reagents and conditions: (a) i—R^3 = Me: HCO_2Et, HCO_2H, reflux, 24 h, 88%; R^3 = Et: Ac_2O, NaOAc, AcOH, 20 °C, 18 h, 99%; R^3 = ^{n}Pr: $(EtCO)_2O$, NaOEt, EtOH, 5–20 °C, 24 h, 70%; R^3 = ^{i}Bu: $(CH_3)_2CHCOCl$, NEt_3, CH_2Cl_2, 0-20 °C, 69%; ii—$BH_3.SMe_2$, THF, 0 °C, reflux, 2 h, 59–84%; or (a) R^3 = ^{i}Pr: acetone, $NaCNBH_3$, MeOH, 0–20 °C, 18 h, 61%; R^3 = ^{c}Pe: cyclopentanone, $NaCNBH_3$, NaOAc, MeOH, 0–20 °C, 2 h, 47%; R^3 = ^{c}Pr: [(1-ethoxycyclopropyloxy)trimethylsilane], NaOAc, $NaCNBH_3$, AcOH, MeOH, 0–50 °C, 2 h, 34%; (b) R^2 = Me: Ac_2O, NaOAc, AcOH, 20–50 °C, 18–48 h, 50–99%; (c) i—H_2 4 bar, 10% Pd/C, EtOH, 20 °C, 3 h; ii—NaOH, EtOH, reflux, 1–4 h, 59–99% (2 steps); (d) DMF-DMA, DMF, 130 °C, 5–72 h, 32–98%.

Table 2
Structures and in vitro activity for imidazoles **4c** and **5**

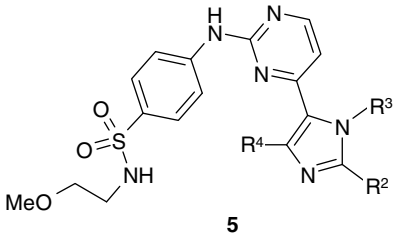

5

Compound	R^2	R^3	R^4	CDK2 IC_{50}[a] (μM)	CDK4 IC_{50}[a] (μM)	LoVo prolif. IC_{50}[b] (μM)
4c	Me	Me	H	0.008	5.6	4.0
5a	Me	Et	H	0.004	1.3	1.5
5b	Me	^{i}Pr	H	0.001	0.20	0.31
5c	Me	^{c}Pe	H	<0.003		0.61
5d	Me	^{i}Bu	H	0.015		1.8
5e	Me	^{c}Pr	H	0.083	>9.0	6.0
5f	Me	Me	Me	0.068	>8.6	9.2

[a] Enzyme protocol Ref. 14.
[b] IC_{50} for inhibition of BrdU incorporation to LoVo cells following 48 h exposure to test compound.

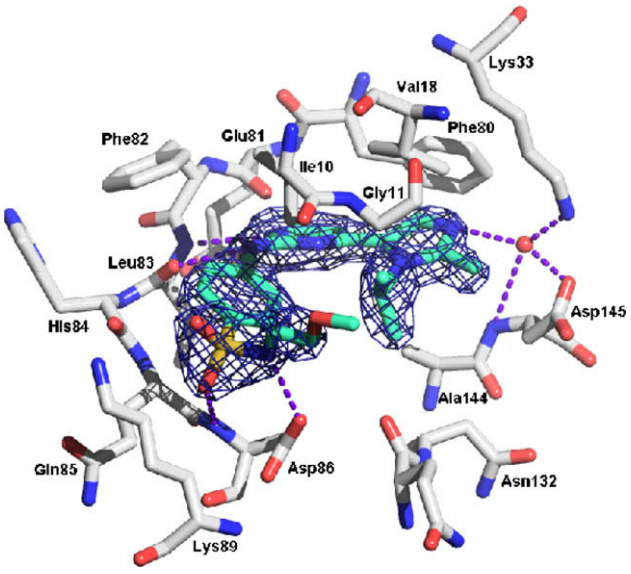

Figure 2. Crystal structure of CDK2 complexed with **5b**[17] showing final $2F_o$-F_c electron density for the inhibitor **5b** (cyan, 1.0σ level). Selected nearby protein residues are shown. Hydrogen bonding interactions with the protein are indicated as dashed purple lines. The figure was prepared using PyMOL.[18]

the compounds retained the other key hydrogen bonding interactions, and the hydrophobic interaction of the α-branched R^3 substituent. Alkylation of the sulfonamide N reduced enzyme activity by approximately 50-fold (Table 1, compare **4f** with **4c**) and increased lipophilicity. Replacement of the sulfonamide with a sulfone also reduced enzyme activity (Table 3, compare **4e** with **6a**), but this could be improved by the use of α-branched R^3 substituents (compare **6b** with **6c**[26,27] and **6a** with **6h**), and alkyl sulfones (compare **6c** and **6d** with **6e**–**6i**). The inclusion of basic substituents tended to reduce CDK2 activity by approximately 6-fold and reduce selectivity for CDK2 over CDK4 to approximately 4-fold (compare **6c** with **6h** and **6i**). The discrepancy between enzyme activity and effects on cellular proliferation is possibly due to sub-optimal cell permeability or serum protein binding.

The physicochemical properties of the imidazole series tended to be superior to those of the imidazo[1,2-*a*]pyridines (**1**) and imidazo[1,2-*b*]pyridazines (**2**) (Table 4). This could be attributed to the reduction in lipophilicity and the replacement of the bicyclic heterocycle with a substituted imidazole (compare **5a** with **2c**). Incorporating basic substituents tended to be required to achieve good physicochemical properties for the imidazo[1,2-*a*]pyridines (compare **1a** with **1c**) and imidazo[1,2-*b*]pyridazines (compare **2c** with **2d**), and also improved the physicochemical properties of the imidazole series (compare **6c** with **6h**).

Compound **6c** displayed a combination of cellular potency and physicochemical properties that made it suitable for further profiling as an orally active CDK inhibitor. Compound **6c** potently inhib-

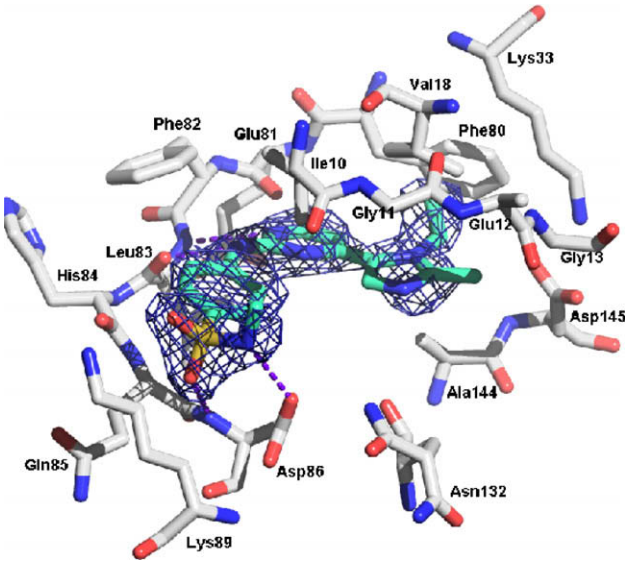

Figure 3. Crystal structure of CDK2 complexed with **5e**[17] showing final $2F_o$-F_c electron density for the inhibitor **5e** (cyan, 1.0σ level). Initial electron density maps showed no evidence for the *N*-ethylmethoxy solubilising group beyond Cβ, and these atoms have therefore been omitted from the model. Selected nearby protein residues are shown. Hydrogen bonding interactions with the protein are indicated as dashed purple lines. The figure was prepared using PyMOL.[18]

Table 3
Structures and in vitro activity for imidazoles **4e** and **6**

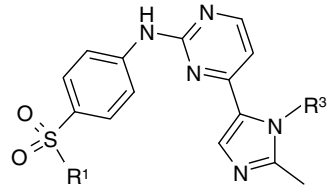

6

Compound	R^1	R^3	CDK2 IC_{50}[a] (μM)	CDK4 IC_{50}[a] (μM)	LoVo prolif. IC_{50}[b] (μM)
4e	$NH(CH_2)_2N(Me)_2$	Me	0.025		
6a	$(CH_2)_3N(Me)_2$	Me	0.295		
6b	Me	Et	0.023		
6c	Me	^{i}Pr	0.006	0.45	0.63
6d	^{n}Pr	^{i}Pr	0.008		1.8
6e	CH_2Ph	^{i}Pr	0.019	1.5	1.5
6f	$(CH_2)_2OMe$	^{i}Pr	0.014	0.49	0.69
6g	CH_2-2-THF	^{i}Pr	0.013	0.53	1.2
6h	$(CH_2)_3N(Me)_2$	^{i}Pr	0.036	0.14	0.89
6i	$(CH_2)_3N(CH_2CH_2)_2O$	^{i}Pr	0.033	0.21	1.2

[a] Enzyme protocol Ref. 14.
[b] IC_{50} for inhibition of BrdU incorporation to LoVo cells following 48 h exposure to test compound.

ited the kinase activity of cyclin E/CDK2, cyclin A/CDK2, cyclin B1/CDK1, cyclin T/CDK9 and cyclin D3/CDK6 (IC_{50} 6, 45, 16, 20 and 21 nM, respectively), and was 75-fold less active against cyclin D/CDK4 and >170-fold selective for CDK2 over a range of other kinases (data not shown). Compound **6c** showed significant blood levels in mice following oral dosing (Table 5), and was selected as a clinical development candidate (AZD5438). Non-clinical in vitro and in vivo pharmacology studies with AZD5438 will be reported elsewhere.

In conclusion, we have discovered an imidazole series of potent CDK inhibitors and we developed a candidate that was progressed into clinical development (**6c**, AZD5438).

Table 4
Structures and physicochemical property summaries for imidazo[1,2-*a*]pyridines **1**, imidazo[1,2-*b*]pyridazines **2** and imidazoles **5a** and **6**

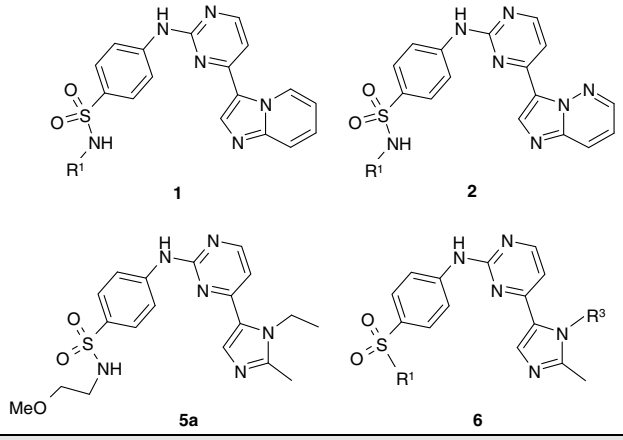

1 **2** **5a** **6**

Compound	R^1	R^3	Log*D* pH 7.4	Solubility pH 7.4, μM	% Free (Rat)
1a	H		2.7	6.5	0.1
1 c	$(CH_2)_2N(Me)_2$		2.7	31	3.0
2c	$(CH_2)_2OMe$		2.8	7.2	0.8
2d	$(CH_2)_3N(Me)_2$		1.4	160	14.8
5a			2.4	53	1.4
6c	Me	^{i}Pr	2.4	218	8.7
6h	$(CH_2)_3N(Me)_2$	^{i}Pr	1.3	>6800	32

Table 5
Mouse PK summary for compound **6c**[a]

Compound	V_{dss}[b] (L/Kg)	Cl[b] (ml/min/Kg)	AUC 0-t[c] (μM h)	C_{max}[c] (μM)	T_{max}[c] (h)	Bioavailability[c] (%)
6c	1.01	21.8	18.7	6.4	0.33	91

[a] Values are average of 2 measurements.
[b] 5.5 mg/Kg iv.
[c] 10 mg/Kg po.

References and notes

1. Malumbres, M.; Barbacid, M. *Trends Biochem. Sci.* **2005**, *30*, 630.
2. Nevins, J. R. *Hum. Mol. Genet.* **2001**, *10*, 699.
3. Shapiro, G. I.; Harper, J. W. *Clin. Invest.* **1999**, *104*, 1645.
4. Hu, B.; Mitra, J.; Van Den, H. S.; Enders, G. H. *Mol. Cell. Biol.* **2001**, *21*, 2755.
5. Ortega, S.; Malumbres, M.; Barbacid, M. *Biochim. Biophys. Acta* **2002**, *1602*, 73.
6. Barton, M. C.; Akli, S.; Keyomarsi, K. *J. Cell. Physiol.* **2006**, *209*, 686.
7. Lopez-Beltran, A.; MacLennan, G. T.; Montironi, R. *Anal. Quant. Cytol.* **2006**, *28*, 111.
8. Senderowicz, A. M. *Prog. Drug Res.* **2005**, *63*, 183.
9. Anderson, M.; Beattie, J. F.; Breault, G. A.; Breed, J.; Byth, K. F.; Culshaw, J. D.; Ellston, R. P. A.; Green, S.; Minshull, C. A.; Norman, R. A.; Pauptit, R. A.; Stanway, J.; Thomas, A. P.; Jewsbury, P. J. *Bioorg. Med. Chem. Lett.* **2003**, *13*, 3021.
10. Byth, K. F.; Culshaw, J. D.; Green, S.; Oakes, S. E.; Thomas, A. P. *Bioorg. Med. Chem. Lett.* **2004**, *14*, 2245.
11. Byth, K. F.; Cooper, N.; Culshaw, J. D.; Heaton, D. W.; Oakes, S. E.; Minshull, C. A.; Norman, R. A.; Pauptit, R. A.; Tucker, J. A.; Breed, J.; Pannifer, A.; Rowsell, S.; Stanway, J.; Valentine, A. L.; Thomas, A. P. *Bioorg. Med. Chem. Lett.* **2004**, *14*, 2249.
12. Byth, K. F.; Geh, C.; Forder, C. L.; Oakes, S. E.; Thomas, A. P. *Mol. Cancer Ther.* **2006**, *5*, 655.
13. Finlay, M. R. V.; Acton, D. G.; Andrews, D. M.; Barker, A. J.; Dennis, M.; Fisher, E.; Graham, M. A.; Green, C. P.; Heaton, D. W.; Karoutchi, G.; Loddick, S. A.; Morgentin, R.; Roberts, A.; Tucker, J. A.; Weir, H. M. *Bioorg. Med. Chem. Lett.* **2008**, *18*, 4442.
14. Thomas, A. P.; Newcombe, N. J.; Heaton, D. W. PCT Int. Application WO 2002004429.
15. Reiter, L. A. *J. Org. Chem.* **1987**, *52*, 2714.
16. Hopkins, A. L.; Groom, C. R.; Alex, A. *Drug Discov. Today* **2004**, *9*, 430.
17. Protein and crystals were obtained according to established procedures.[19,20] Crystals were soaked in 2 mM compound **5b** (5 mM compound **5e**) overnight in mother liquor containing 10% DMSO. Diffraction data were collected on beamline PX14.2 at the SRS, Daresbury, at 100 K (a MarResearch 345 mm image plate using a Bruker Nonius FR591 rotating anode generator operated at 5.5 kW at 100 K for compound **5e**). Data processing, data reduction and

structure solution by molecular replacement were carried out using programs from the CCP4 suite.[21] Compounds **5b** and **5e** were modeled into the electron density using QUANTA.[22] The protein-compound complex models were refined using CNX,[23] and the final structures[24,25] have been deposited in the Protein Data Bank with the deposition codes 2w05 (**5b**) and 2w06 (**5e**) together with structure factors and detailed experimental conditions.

18. DeLano, W. L. The PyMOL molecular graphics system **2003**, DeLano Scientific, San Carlos, CA, http://www.pymol.org
19. Lawrie, A. M.; Noble, M. E.; Tunnah, P.; Brown, N. R.; Johnson, L. N.; Endicott, J. A. *Nat. Struct. Biol.* **1997**, *4*, 796.
20. Legraverend, M.; Tunnah, P.; Noble, M.; Ducrot, P.; Ludwig, O.; Grierson, D. S.; Leost, M.; Meijer, L.; Endicott, J. *J. Med. Chem.* **2000**, *43*, 1282.
21. CCP4 *Acta Crystallogr*. **1994**, *D50*, 760.
22. Quanta2000, Accelrys.
23. CNX version 2000.1, Accelrys.
24. Crystallographic statistics for the CDK2-compound **5b** complex are as follows: space group $P2_12_12_1$, unit cell 53.1, 70.3, 71.7 Å, resolution 1.90 Å, 19,692 reflections from 43,397 observations give 91.0% completeness with R_{merge} of 7.2% and mean I/σ *(I)* of 8.0. The final model containing 2184 protein, 124 water, and 30 compound atoms has an *R*-factor of 22.9% (R_{free} using 5% of the data 29.3%). Mean temperature factors for the protein and the ligand are 35.3 and 33.3 Å^2 respectively.
25. Crystallographic statistics for the CDK2-compound **5e** complex are as follows: space group $P2_12_12_1$, unit cell 53.6, 72.6, 71.9 Å, resolution 2.04 Å, 17,949 reflections from 52,641 observations give 97.5% completeness with R_{merge} of 4.6% and mean I/σ *(I)* of 15.6. The final model containing 2237 protein, 141 water, and 27 compound atoms has an R-factor of 20.5% (R_{free} using 5% of the data 23.4%). Mean temperature factors for the protein and the ligand are 31.0 and 34.6 Å^2 respectively.
26. Compound **6c**: NMR (DMSO-d_6) δ1.52 (d, 6H), 2.79 (s, 3H), 3.14 (s, 3H), 5.56 (m, 1H), 7.28 (d, 1H), 7.83 (d, 2H), 7.96 (d, 2H), 8.20 (s, 1H), 8.71 (d, 1H), 10.28 (s, 1H); MS 372 $[MH]^+$.
27. Synthesis protocol for compounds **6c**, **6e**, and **6g–6i**: Newcombe, N. J.; Thomas, A. P. PCT Int. Application WO 2003076436.